Development of multiplex allele-specific RT-qPCR assays for differentiation of SARS-CoV-2 Omicron subvariants

Jianguo Li[1] · Ruiling Cheng[1] · Zixin Bian[2] · Jiahui Niu[1] · Juan Xia[1] · Guoli Mao[3] · Hulong Liu[3] · Changxin Wu[1] · Chunyan Hao[4]

Abstract

Quick differentiation of current circulating variants and the emerging recombinant variants of SARS-CoV-2 is essential to monitor their transmissions. However, the widely applied gene sequencing method is time-consuming and costly especially when facing recombinant variants, because a large part or whole genome sequencing is required. Allele-specific reverse transcriptase real time RT-PCR (RT-qPCR) represents a quick and cost-effective method for SNP (single nucleotide polymorphism) genotyping and has been successfully applied for SARS-CoV-2 variant screening. In the present study, we developed a panel of 5 multiplex allele-specific RT-qPCR assays targeting 20 key mutations for quick differentiation of the Omicron subvariants (BA.1 to BA.5 and their descendants) and the recombinant variants (XBB.1 and XBB.1.5). Two parallel multiplex RT-qPCR reactions were designed to separately target the prototype allele and the mutated allele of each mutation in the allele-specific RT-qPCR assay. Optimal annealing temperatures, primer and probe dosage, and time for annealing/extension for each reaction were determined by multi-factor and multi-level orthogonal test. The variation of Cp (crossing point) values (ΔCp) between the two multiplex RT-qPCR reactions was applied to determine if a mutation occurs or not. SARS-CoV-2 subvariants and related recombinant variants were differentiated by their unique mutation patterns. The developed multiplex allele-specific RT-qPCR assays exhibited excellent analytical sensitivities (with limits of detection (LoDs) of 1.47–18.52 copies per reaction), wide linear detection ranges (10^9–10^0 copies per reaction), good amplification efficiencies (88.25 to 110.68%), excellent reproducibility (coefficient of variations (CVs) < 5% in both intra-assay and inter-assay tests), and good clinical performances (99.5–100% consistencies with Sanger sequencing). The developed multiplex allele-specific RT-qPCR assays in the present study provide an alternative tool for quick differentiation of the SARS-CoV-2 Omicron subvariants and their recombinant variants.

Key points

● A panel of five multiplex allele-specific RT-qPCR assays for quick differentiation of 11 SARS-CoV-2 Omicron subvariants (BA.1, BA.2, BA.4, BA.5, and their descendants) and 2 recombinant variants (XBB.1 and XBB.1.5).
● The developed assays exhibited good analytical sensitivities and reproducibility, wide linear detection ranges, and good clinical performances, providing an alternative tool for quick differentiation of the SARS-CoV-2 Omicron subvariants and their recombinant variants.

✉ Jianguo Li
lijg@sxu.edu.cn

✉ Chunyan Hao
haochunyan@126.com

1 Shanxi Provincial Key Laboratory of Medical Molecular Cell Biology, Institutes of Biomedical Sciences, Shanxi University, Taiyuan 030006, People's Republic of China

2 College of Life Sciences, Shanxi University, Taiyuan 030006, People's Republic of China

3 Shanxi Guoxin Caregeno Biotechnology Co., Ltd., Taiyuan 030032, People's Republic of China

4 School of Environment and Resources, Taiyuan University of Science and Technology, Taiyuan 030024, People's Republic of China

Introduction

The current circulating Omicron variant of SARS-CoV-2 has diverged into at least five subvariants (BA.1, BA.2, BA.3, BA.4, and BA.5) with emerging sub-lineages as their descendants (World Health Organization 2021). To gain stronger transmissibility and more immune escape chances, the Omicron variant continues evolving, leading to emerging descendent sub-lineages with varied genetic constellations of mutations (Becker et al. 2021). Each sub-lineage containing differed genetic constellation may pose different public health risk (Islam et al. 2022). Thus, further investigations are required to access their characteristics diverged from the parental variants (Oude Munnink and Koopmans 2023). As of April 1, 2023, a total of four Omicron sub-lineages were under monitoring by the World Health Organization (WHO), including BF.7, BQ.1, BA2.75, and XBB recombinant variants (World Health Organization 2021).

Unique genetic constellations of Omicron subvariants have been identified, including those for BA.1 (NSP3: L1266I; NSP6: I189V; Spike: S371L, G446S, T547K, and L981F) (Yu et al. 2022), BA.2 (NSP1: S135R, NSP3: T24I, NSP6: F108L, Spike: A27S, V213G, and R408S) (Majumdar and Sarkar 2022), BA.4 (N: P151S, ORF1ab: K141-F143del), and BA.5 (M: D3N, ORF1ab: L3027del) (Wolter et al. 2022). The Omicron sub-lineages under WHO monitoring were identified with additional genetic mutations (World Health Organization 2021), including BF.7 (BA.5 + Spike: R346T+N: [G30- + S33F] + ORF9b: [M26- + A29I + V30L]), BQ.1 (BA.5 + Spike: [R346T + K444T + N460K]+ ORF1a: [Q556K + L3829F] + ORF1b: [Y264H + M1156I + N1191S] + N: E136D + ORF9b: P10F), BA.2.75 (BA.2 + Spike: [K147E + W152R + F157L + I210V + G257S + D339H + G446S + N460K + Q493R reversion] + ORF1a: [S1221L + P1640S + N4060S] + ORF1b: G662S + E: T11A), and the recombinant variant XBB (from BA.2.75 and BA.2.10.1) and XBB.1.5 (XBB + Spike: F486P).

Although gene sequencing represents the golden standard assay for viral variant identification, differentiation of massive variants by sequencing is time-consuming and costly (Srivastava et al. 2021). Allele-specific real-time RT-PCR (RT-qPCR), a highly sensitive and time-saving method for SNP (single nucleotide polymorphism) genotyping (Germer and Higuchi 2003), has been successfully applied for identification of SARS-CoV-2 mutations, exhibiting an excellent potential in differentiation of viral variants (Graber et al. 2021; Wang et al. 2021).

In the present study, we developed a panel of five multiplex allele-specific RT-qPCR assays with primer design using the similar principle introduced by Germer and Higuchi (2003), targeting 20 key mutations for differentiation of the Omicron subvariants and related recombinant variants.

Materials and methods

Ethical statement

The application of desensitized clinical specimens for evaluation of the developed allele-specific RT-qPCR assays was approved by the Ethics Committee of Shanxi University with a projection identification code SXULL2022057.

Viral genome sequence analysis and primer/probe design

A total of 3631 genome sequences of SARS-CoV-2 Omicron subvariants with high quality (<1% Ns) deposited in GISAID (https://www.gisaid.org) were retrieved. Sequence alignment was performed by using the Muscle algorithm implemented in MEGA v7.0 (Kumar et al. 2016). The key mutations in Omicron subvariants and related recombinant variants were confirmed, and viral genomic regions suitable for primer/probe design were selected (Table 1) by the help of Primer Express v3.0 (Applied Biosystems, Foster, CA, USA). Primers and probe were designed according to the following principles: avoiding regions with complex secondary structure, with an amplicon of 100–220 bp, choosing regions with GC content of 40–60%, avoiding regions with long (>4) repeats of single bases, avoiding the guanine (G) at the 5′ end of probes, all of the selected primers have similar melting temperature (Tm, between 59 and 61 °C), and Tms of the corresponding probes were 5–10 °C higher.

Plasmid construction and RNA transcript preparation

A plasmid pEasy-T1 (TransGen Biotech, Beijing, China), incorporating with a viral gene (*spike* [S], *nucleocapsid* [N], *matrix* [M], or *envelope* [E]) was linearized by digestion with restriction enzyme for RNA transcript preparation by using the RiboMAX^TM Large Scale RNA production System (Promega, Mfadison, WI, USA) according to the manufacturer's instructions. Concentrations of the RNA transcript were measured by using NanoDrop (Thermo Fisher Scientific, MA, USA). Copy number of the transcript was calculated with the following formula: Copy number (copies/ml) = 6.02×10^{23} copies/mol × molarity (mol/L)/molecular weight (g/mol). The quantified RNA transcript was then 10-fold diluted with RNase-free water as templates for development of the allele-specific RT-qPCR assays.

Table 1 Primers and probes for the developed multiplex allele-specific RT-qPCR assays

Assay		Allele	Forward primer (5′-3′)	Probe (5′-3′)	Reverse primer (5′-3′)	Amplicon (bp)
Prototype allele targeting reactions	Assay 1	S: T95I	TGATGGTGTTTATTTTGCTTCCAC	CTGGATTTTTGGTACTACTTTAGATTCGAAGACCCAGT	GTGGTAATAAACACCCAAAAATGGATC	177
		N: P151S	CATTGGCACCCGCAATC	CCTGCTAACAATGCTGCAATCGTGCTACA	CTGCCTGGAGTTGAATTTCTTG	167
		S: T547K	TGTGTCAATTTCAACTTCAATGGTTTAAC	CAGGCACAGGTGTTCTTACTGAGTCTAACAAAAGTTTC	CCAAAAGAACATGGTGTAATGTCAAG	166
		S: N460K	GGTAATTATAATTACCTGTATAGAATTGTTTAGGAAGTCTAAT	CAACTGAAATCTATCAGGCCGGTAGCACAC	GGTTGGAAACCATATGATTGTAAAGG	157
	Assay 2	S: T19I	CTAGTCTCTAGTCAGTGTGTTAATCTTAC	CAACCAGAACTCAATTACCCCCTGCATACAC	TAAGAACAAGTCCTGAGTTGAATGT	141
		S: S704L	ACTATGTCACTTGGTGCAGAAAATTC	CCACAGAAATTCTACCAGTGTCTATGACCAAGACATCA	GTGTACAAAAACTGCCATATTGCAAC	173
		S: S371F	CTGTGTTGCTGATTATTCTGTCCTATATAATTC	CCGCATCATTTTCCACTTTTAAGTGTTATGGAGTGTCT	CGATTTGTCTGACTTCATCACCTCTAA	151
		S: D405N	GTCTATGCAGATTCATTTGTAATTAGAGGTG	CAGACAAATCGCTCCAGGGCAAACTG	TGAGATTAGACTTCCTAAACAATCTATACAGG	201
	Assay 3	S: Δ24-26A27S	CCAGAACTCAATTACCCCCTG	CATACACTAATTCTTCACACGTGGTGTTTATTACCCTGA	GCATGGAACCAAGTAACATTGG	141
		S: F486V	CACCTTGTAATGGTGTTGAAGGTT	CCAACCCACTAATGGTGTTGGTTACCAACC	CTGTTAAACCATTGAAGTTGAAATTGACAC	186
		S: S37IL	CTGTGTTGCTGATTATTCTGTCCTATATAATTC	CCGCATCATTTTCCACTTTTAAGTGTTATGGAGTGTCT	GATTTGTCTGACTTCATCACCTCTAA	150
		S: L452R	TGATTCTAAGGTTGGTGGTAATTATAATTACCT	TTGAGAGAGATATTTCAACTGAAATCTATCAGGCCGGTAGC	CCATTAGTGGGTTGGAAACCATATG	182
	Assay 4	E: T11A	TCGTTTCGAAGAGACAGGTA	TCGTGGTATTCTTGCTAGTTACACTAGCCATCCTTAC	AGAAGATCAGGAACTCTAGAAGAATTCAG	210
		M: D3N	GGAACTTTAATTTTAGCCATGGCAG	CCAACGGTACTATTACCGTTGAAGAGCTTAAAAAGC	TTGGCATAGGCAAATTGTAGAAGAC	139
		S: N856K	ACCTCATTTGTGCACAAAAGTTTAAC	CGGCCTTACTGTTTTGCCACCTTTGC	CTATAAGCCATTTGCATAGCAAATGG	146
		S: L452Q	TGATTCTAAGGTTGGTGGTAATTATAATTACCT	TTGAGAGAGATATTTCAACTGAAATCTATCAGGCCGGTAGC	CCATTAGTGGGTTGGAAACCATATG	182
	Assay 5	S: K147E	GATCCATTTTTGGGTGTTATTACCACA	CTCTCAGCCTTTTCTTATGGACCTTGAAGGAAAACAG	CACTAAATTAATAGGCGTGTGCTTAG	227
		S: I210V	GGTTATTTTAAAATATATTCTAAGCACACGCCTA	TAGTGCGGTGATCCTCCCTCAGGGTTTTTCG	GAAATCACCAGGAGTCAAATAACTTCTATG	166
		S: G257S	GACTCCTGGTGATTCTTCTTCAG	TTGGACAGCTGGTGCTGCAGCTTAT	CAGTGAAGGATTTCAACGTACACT	175
		S: F486P	CACCTTGTAATGGTGTTGAAGGTT	CCAACCCACTAATGGTGTTGGTTACCAACC	CTGTTAAACCATTGAAGTTGAAATTGACAC	209
Mutated allele targeting reactions	Assay 1	S: T95I	TGATGGTGTTTATTTTGCTTCCAT	CTGGATTTTTGGTACTACTTTAGATTCGAAGACCCAGT	GTGGTAATAAACACCCAAAAATGGATC	177
		N: P151S	ACATTGGCACCCGCAATT	TCTGCTAACAATGCTGCAATCGTGCTACAAC	CTGCCTGGAGTTGAATTTCTTG	168

Table 1 (continued)

Assay	Allele	Forward primer (5'-3')	Probe (5'-3')	Reverse primer (5'-3')	Amplicon (bp)
	S: T547K	ATGTGTCAAITTCAACTTCAATGGTTTAAA	AAGGCACAGGTGTTCTTACTGAGTCTAACAAAAGT	CCAAAAGAACATGGTGTAATGTCAAG	167
	S: N460K	GGTAATTATAATTACCTGTATAGAITGTTTAGGAAGTCTAAG	CAACTGAAATCTATCAGGCCGGTAGCACAC	GGTTGGAAACCATATGATTGTAAAGG	157
Assay 2	S: T19I	ACTAGTCTCTAGTCAGTGTGTTAATCTTAT	TAACCAGAACTCAATTACCCCCTGCATACAC	TAAGAACAAGTCCTGAGTTGAATGT	142
	S: S704L	ACTATGTCACTTGGTGCAGAAAAATTT	CCACAGAAATTCTACCAGTGTCTATGACCAAGACATCA	GTGTACAAAAACTGCCATATTGCAAC	173
	S: S371F	ACTGTGTTGCTGATTATTCTGTCCTATATAAITTT	CCGCATCAITTTCCACTTTTAAGTGTTATGGAGTGTCT	CGATTTGTCTGACTTCATCACCTCTAA	152
	S: D405N	TGTCTATGCAGATTCAITTGTAATTAGAGGTA	CAGACAAATCGCTCCAGGGCAAACTG	TGAGATTAGACTTCCTAAACAATCTATACAGG	202
Assay 3	S: Δ24-26A27S	TGTGTTAATCTTACAACCAGAACTCAAT	CATACACTAAITCTTTCACACGTGGTGTTTATTACCCTGA	GCATGGAACCAAGTAACATTGG	130
	S: F486V	ACCTTGTAATGGTGTTGAAGGTG	CCAACCCACTAATGGTGTTGGTTACCAACC	CTGTTAAACCATTGAAGTTGAAATTGACAC	185
	S: S371L	TGTGTTGCTGATTATTCTGTCCTATATAAATCT	TCGCATCAITTTCCACTTTTAAGTGTTATGGAGTGTCTCC	GAITTGTCTGACTTCATCACCTCTAA	150
	S: L452R	GAITCTAAGGTTGGTGGTAATTATAATTACCG	TTGAGAGAGATATTTCAACTGAAATCTATCAGGCCGGTAGC	CCATTAGTGGGTTGGAAACCATATG	181
Assay 4	E: T11A	CGTTTCGGAAGAGAGACAGGTG	TCGTTGGTATTCTTGCTAGTTACACTAGCCATCCTTAC	AGAAGATCAGGAACTCTAGAAGAATTCAG	209
	M: D3N	TGGAACTTTAAITTTAGCCATGGCAA	CCAACGGTACTATTACCGTTGAAGAGCTTAAAAAGC	TTGGCATAGGCAAATTGTAGAAGAC	140
	S: N856K	GACCTTCAITTGTGCACAAAAGTTTAAA	AGGCCTTTACTGTTTTGCCACCTTTGC	CTATAAGCACATTTGCATAGCAAATGG	147
	S: L452Q	TGAITCTAAGGTTGGTGGTAATTATAATTACCA	TTGAGAGAGATATTTCAACTGAAATCTATCAGGCCGGTAGC	CCATTAGTGGGTTGGAAACCATATG	182
Assay 5	S: K147E	CCATTTTTGGGGTGTTTATTACCACG	CTCTCAGCCTTTTCTTATGGACCTTGAAGGAAAACAG	CACTAAATTAATAGGCGTGTGCTTAG	224
	S: I210V	GTTAITTTAAAATATATTCTAAGCACACGCCTG	TAGTGCGTGATCTCCCTCAGGGGTTTTTCG	GAATCACCAGGAGTCAAATAACTTCTATG	165
	S: G257S	TGACTCCTGGTGAITCTTCTTCAA	TTGGACAGCTGGTGCTGCAGCTTAT	CAGTGAAGGAITTTCAACGTACACT	176
	S: F486P	ACCTTGTAATGGTGTTGAAGGTG	CCAACCCACTAATGGTGTTGGTTACCAACC	CTGTTAAACCATTGAAGTTGAAATTGACAC	208

Formulation and procedures of the developed multiplex allele-specific RT-qPCR assays

The multiplex RT-qPCR assays were developed by using Takara OneStep PrimeScript[TM] III RT-qPCR Mix (Takara, Dalian, China). Each reaction mix consisted of 10 µl OneStep PrimeScript[TM] III RT-qPCR Mix, optimal dosages of four primers and probe sets, 2 µl RNA template, and supplemented with RNase-free water to a final volume of 20 µl. Dosage for primers and probe sets was tested by using serial dilutions, annealing temperatures were tested by using thermal-gradient experiments, and time for annealing/extension was tested by serial time points. Optimal reaction conditions were determined by multi-factor and multi-level orthogonal test (Raso et al. 2011). Fluorescence acquisition was set at the annealing/extension step of each cycle. Each reaction was run in triple replicates with 96-well plates by a Roche LightCycler 480 (Roche, Indianapolis, IN, USA).

Methodological evaluations of the developed multiplex allele-specific RT-qPCR assays

Ten-fold dilutions of in vitro transcribed RNA of the viral genes were applied for methodological evaluations of the developed allele-specific RT-qPCR assays. Fitting curves generating from the quantity of RNA transcripts and the corresponding Cp (crossing point) values were applied for determination of the linear detection ranges of the RT-qPCR assays. Correlation coefficient (R^2) in the fitting curve (ranging from 0 to 1, with the value closer to 1 suggesting higher linearity) was applied for evaluation of the detection linearity, with the threshold for good linearity defined as $R^2 > 0.99$. Amplification efficiencies of the RT-qPCR assays were calculated by the slope of the fitting curve, defined as $[10^{(-1/slope)}]-1$. The value of amplification efficiency ranges from 0 to 1, with a value closer to 1 indicating a higher amplification efficiency. Reproducibility of the multiplex allele-specific RT-qPCR assays was evaluated by using the parameter "coefficient of variation (CV)," which was calculated by the standard deviation of a Cp value for an RNA dilution divided by the mean Cp values for all replicates of the same RNA dilution. Intra-assay and inter-assay reproducibility were assessed by triple replicates in one run and three runs in three days, respectively. Limit of detection (LoD, defined as the minimum detected concentration at 95% probability) for each RT-qPCR assay was determined through the Probit regression analysis implemented in SPSS v22.0 (IBM, Chicago, IL, USA) by using a series of 2-fold diluted RNA transcript.

Clinical performance of the developed multiplex allele-specific RT-qPCR assays

Oropharyngeal swabs were applied for evaluation of performance of the developed multiplex allele-specific RT-qPCR assays. Sample size was determined by using PASS v1.5 (KCSS, Kaysville, UT, USA) with the following settings: expected sensitivity at 95%, expected specificity at 99%, tolerated error for specificity at 10%, and confidence level (1-α) at 0.95. A volume of 20 µl RNA was extracted from 200 µl of each swab containing viral transport medium by using the Trizol RNA extraction method (Rio et al. 2010). SARS-CoV-2 nucleic acid detection was performed by using a previously reported assay (Liu et al. 2020; Xiao et al. 2021), and the corresponding viral variant/subvariant was confirmed by Sanger sequencing.

Multiple parameters were applied for evaluating the clinical performance of the developed assays, including clinical sensitivity (the probability of a positive test result), clinical specificity (the probability of a negative result), positive predictive value (PPV, the proportion of subjects with a positive test result who truly positive determined by Sanger sequencing), negative predictive value (NPV, the proportion of subjects with a negative test result who truly negative determined by Sanger sequencing), Youden index (the overall discriminative power of an assay against the golden standard assay), Kappa index, and agreement rate (the extent of agreement between two assays).

Results

Design and reaction condition optimization for developing multiplex allele-specific RT-qPCR assays

A panel of 5 multiplex allele-specific RT-qPCR assays targeting 20 key mutations were developed for differentiation of the SARS-CoV-2 Omicron subvariants (BA.1, BA.2, BA.4, BA.5, and their descendants) and related recombinant variants (XBB.1 and XBB.1.5). Each assay contained two parallel reactions targeting the prototype allele and the corresponding mutated allele of each mutation, respectively. Each reaction contained 4 TaqMan hydrolysis probes targeting 4 mutations, labeled with 5′-FAM-BHQ1-3′, 5′-VIC-BHQ1-3′, 5′-CY3-BHQ2-3′, and 5′-CY5-BHQ2-3′, respectively (Table 1). The forward primer was designed to be allele specific, with one additional mutation at the 3′ terminus to amplify the mismatch effect (Fig. 1a).

Reaction conditions, including dosage of primers and probe set, time for annealing/extension, and annealing
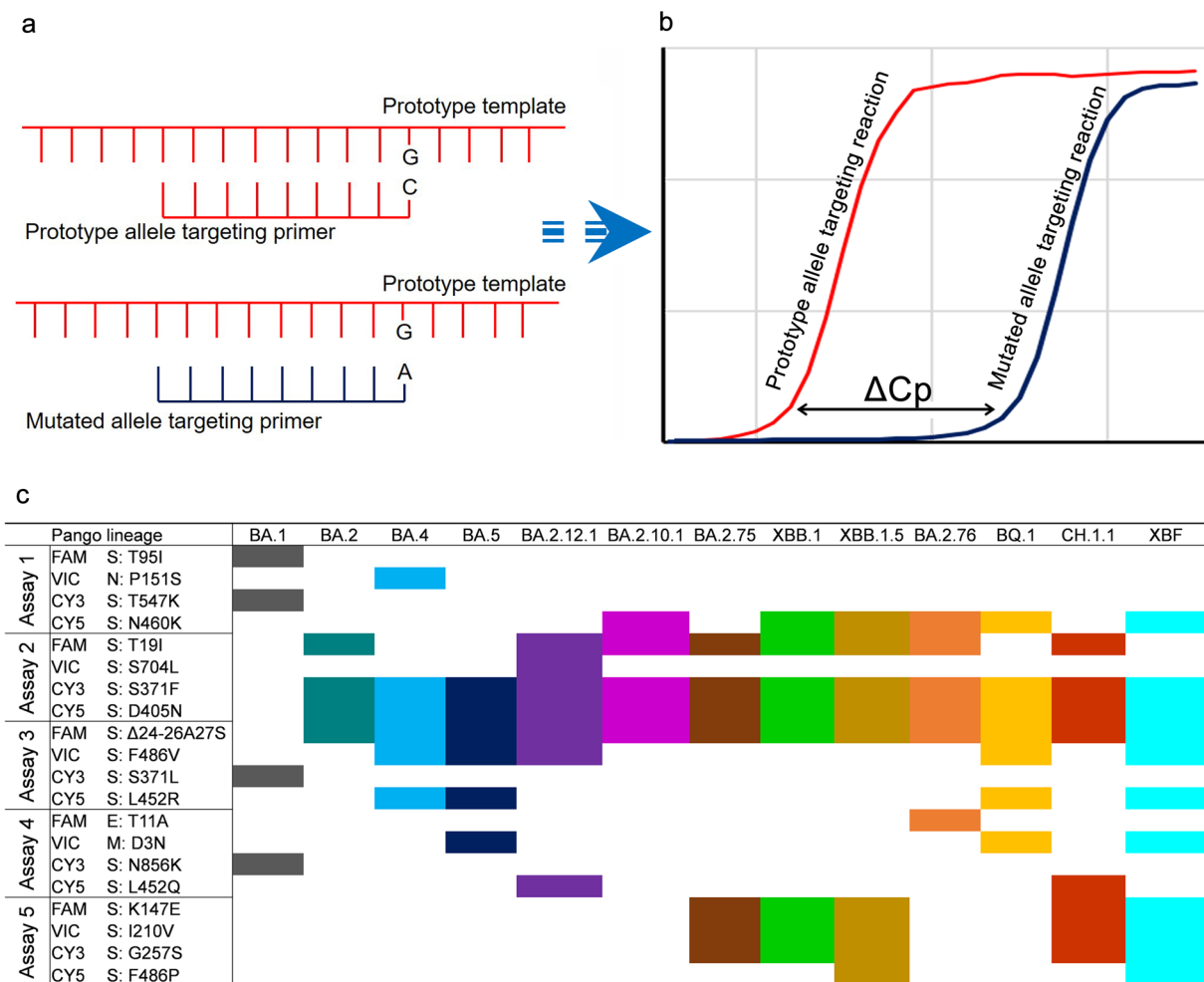
Fig. 1 The principle and covered viral mutations of the developed multiplex allele-specific RT-qPCR assays. **a** Principle for primers and probe design of the developed RT-qPCR assays. Each assay consisted prototype allele targeting and mutated allele targeting reactions. The forward primer for prototyping allele differed from that for mutated allele at the 3′ end. Mismatch between prototype allele targeting reaction and the mutated template (or mismatch between mutated allele targeting reaction and the prototype template) was applied for differentiation of prototype allele and mutated allele. **b** The variation of Cp values (ΔCp) generated from mismatch between the primer and template was used for determination if a mutated allele exists in the tested template. **c** A total of 20 mutations were enrolled for differentiation of SARS-CoV-2 Omicron subvariants and related subvariants. Viral variant differentiation was performed by comparing the detected mutations with the unique mutation patterns for each variant. The Pango nomenclature is widely accepted by researchers and public health agencies worldwide for classifying and naming genetically distinct lineages of SARS-CoV-2, including variants of concern, and is based on the analysis of complete or near-complete virus genomes

temperature, were tested for each reaction in the developed assays. A serial dilution from 0.2 to 0.05 μM was applied for primers and probe dosage (Supplemental Fig. S1). A series of time points from 30 to 60 s were applied for annealing/extension time (Supplemental Fig. S2). A series of thermal gradients from 59 to 61 °C were applied for annealing temperature (Supplemental Fig. S3). Optimal conditions were determined by using three-factor and three-level orthogonal test, with the choice of smaller Cp values corresponded multifactor combinations as the optimal reaction conditions (Supplemental Table S1).

Result interpretation of the developed multiplex allele-specific RT-qPCR assays

The variation of Cp values (ΔCp) between the two parallel reactions induced by primer-target mismatch was employed to differentiate the prototype allele and the mutated allele (Fig. 1b). A mutation should not occur when the Cp value for the prototype allele was smaller than that for the mutated allele. A mutation was determined to occur if the Cp value in the mutated allele targeting reaction was smaller than that in the prototype allele targeting reaction. The threshold was set

as $\Delta Cp > 2$ according to the performance of all the 5 developed assays. If $\Delta Cp \leq 2$, a repeated test should be performed to confirm the result. The mutation will be denied if $\Delta Cp \leq 2$ is confirmed. From the results of prototype template targeting and mutated template targeting reactions by using prototype template (Fig. 2) and mutated template (Fig. 3), the ΔCp values for prototype templates of the developed assays ranged from 2.22 to 39.41 (Table 2), and those for mutated templates ranged from 2.48 to 39.24 (Table 2). The presence of a viral variant was determined by comparing all the detected mutations with the unique mutation patterns for viral variants as shown in Fig. 1c. These results suggested that the developed assays were suitable for differentiation of SARS-CoV-2 Omicron subvariants and related recombinant variants.

Analytical sensitivities of the developed multiplex allele-specific RT-qPCR assays

The analytical sensitivity of the developed RT-qPCR assay was represented by limit of detection (LoD). LoD, defining as the minimum detected template concentration at 95% probability, was calculated by the Probit regression analysis implemented in SPSS 22.0 (IBM Corp (2013)). Using a 2-fold serially diluted in vitro transcribed RNA (from 100 to 0.1 copies per reaction) as templates, the LoDs for the prototype allele targeting reactions of the developed multiplex allele-specific RT-qPCR assays were determined to be 1.47–8.99 copies per reaction (Supplemental Table S2, Fig. 4), while the LoDs for the mutated allele targeting reactions were 1.73–18.52 copies per reaction (Supplemental Table S2, Fig. 5). These results suggested excellent analytical sensitivities of the developed multiplex allele-specific RT-qPCR assays.

Linear detection ranges and amplification efficiencies of the developed multiplex allele-specific RT-qPCR assays

Linear detection range serves as one of the key indicators for RT-qPCR performance, which is defined as the span of signal intensities that display a linear relationship between quantity of RNA transcript and the corresponding Cp values. By using the 10-fold diluted in vitro transcribed RNA as templates, the linear detection range of the developed multiplex allele-specific RT-qPCR assays was determined with the parameter correlation coefficient (R^2, ranging from 0 to 1, the value closer to 1 represents stronger relationship). In the prototype allele targeting reactions (Table 3), the linear detection ranges were 10^9–10^0 copies per reaction ($R^2 > 0.99$) for most of the targeted alleles, while those for the alleles of N: P151S, S: T19I, and S: F486V were 10^9–10^{-1} copies per reaction ($R^2 > 0.99$). In the mutated

allele targeting reactions (Table 4), the linear detection ranges were 10^9–10^{-1} copies per reaction ($R^2 > 0.99$) for most of the targeted alleles, while those for the alleles M: D3N, S: N856K, S: K147E, S: I210V, S: G257S, and S: F486P were 10^9–10^0 copies per reaction ($R^2 > 0.99$).

Amplification efficiency is defined as the ratio of actual amplicon number to theoretical amplicon number from the same original template, with an efficiency value of 100% representing two copies of amplicon generated from one available template. We tested the amplification efficiency of the developed assay by using the 10-fold diluted in vitro transcribed RNA with triple replicates. The amplification curves for both of the prototype allele targeting reactions (Fig. 2) and the mutated allele targeting reactions (Fig. 3) exhibited approximately equal interval, indicating good amplification efficiencies of the developed assays. We further calculated the amplification efficiencies by using the formula: amplification efficiency = $10^{(-1/\text{slope})} - 1$, in which slope is the slope of the fitting curve between the quantity of RNA transcript and the corresponding Cp values. The amplification efficiencies were ranged from 88.25 to 110.68% for the prototype allele-targeting reactions (Table 4) and ranged from 89.57 to 105.82% for the mutated allele-targeting reactions (Table 4). These results demonstrated wide linear detection ranges and good amplification efficiencies of the developed multiplex allele-specific RT-qPCR assays.

Reproducibility of the developed multiplex allele-specific RT-qPCR assays

The intra-assay and inter-assay reproducibility of the developed RT-qPCR assays were separately assessed by coefficient of variation (CV) between quantity of RNA template and the corresponding Cp values in triplicate repeated tests. For the intra-assay reproducibility (Supplemental Table S3), the CVs were 0.00–4.53 in the prototype allele targeting reactions and were 0.03–4.53 in the mutated allele targeting reactions. For the inter-assay reproducibility (Supplemental Table S4), the CVs were 0.00–4.82 in the prototype allele targeting reactions and were 0.04–4.85 in the mutated allele targeting reactions. These results suggested excellent intra- and inter-assay reproducibility (with coefficient of variation less than 5%) of the developed multiplex allele-specific RT-qPCR assays.

Clinical performance of the developed multiplex allele-specific RT-qPCR assays

A minimum of 94 clinical specimens were required to evaluated the clinical performance of the developed assays, determined by setting the expected sensitivity as 95%, the expected specificity as 99%, tolerated error for specificity as 10%, confidence level (1- α) as 0.95. Thus, a total of 113 throat
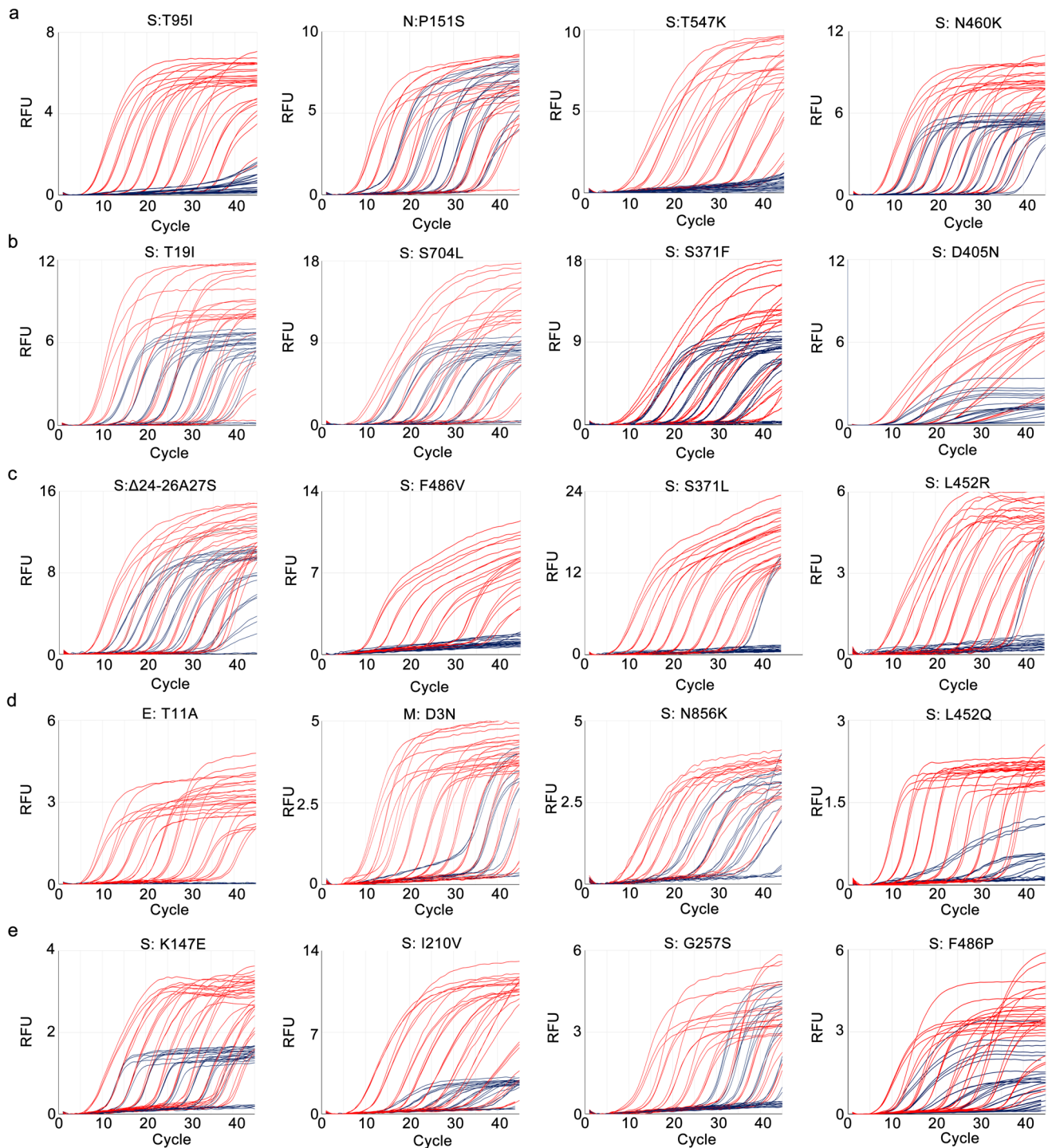
Fig. 2 Amplification curves for the developed multiplex allele-specific RT-qPCR assays against the prototype genes of SARS-CoV-2. The viral prototype genes were in vitro transcribed and 10-fold diluted from 10^9 copies/reaction (2.57×10^9, 4.28×10^9, 3.32×10^9, and 6.61×10^9 for *nucleocapsid*, *envelope*, *membrane*, and *spike*, respectively) to 10^{-1} copies/reaction. Two parallel reactions targeting the prototype allele and the mutated allele of the developed assays were performed by using the in vitro transcribed and serially diluted prototype RNA as template. The amplification curves for the prototype allele-targeting reactions (in red) were then merged with those of the corresponding mutated allele-targeting reactions (in dark blue). RFU, relative fluorescence units, is a measurement of the fluorescence intensity generated from real-time PCR
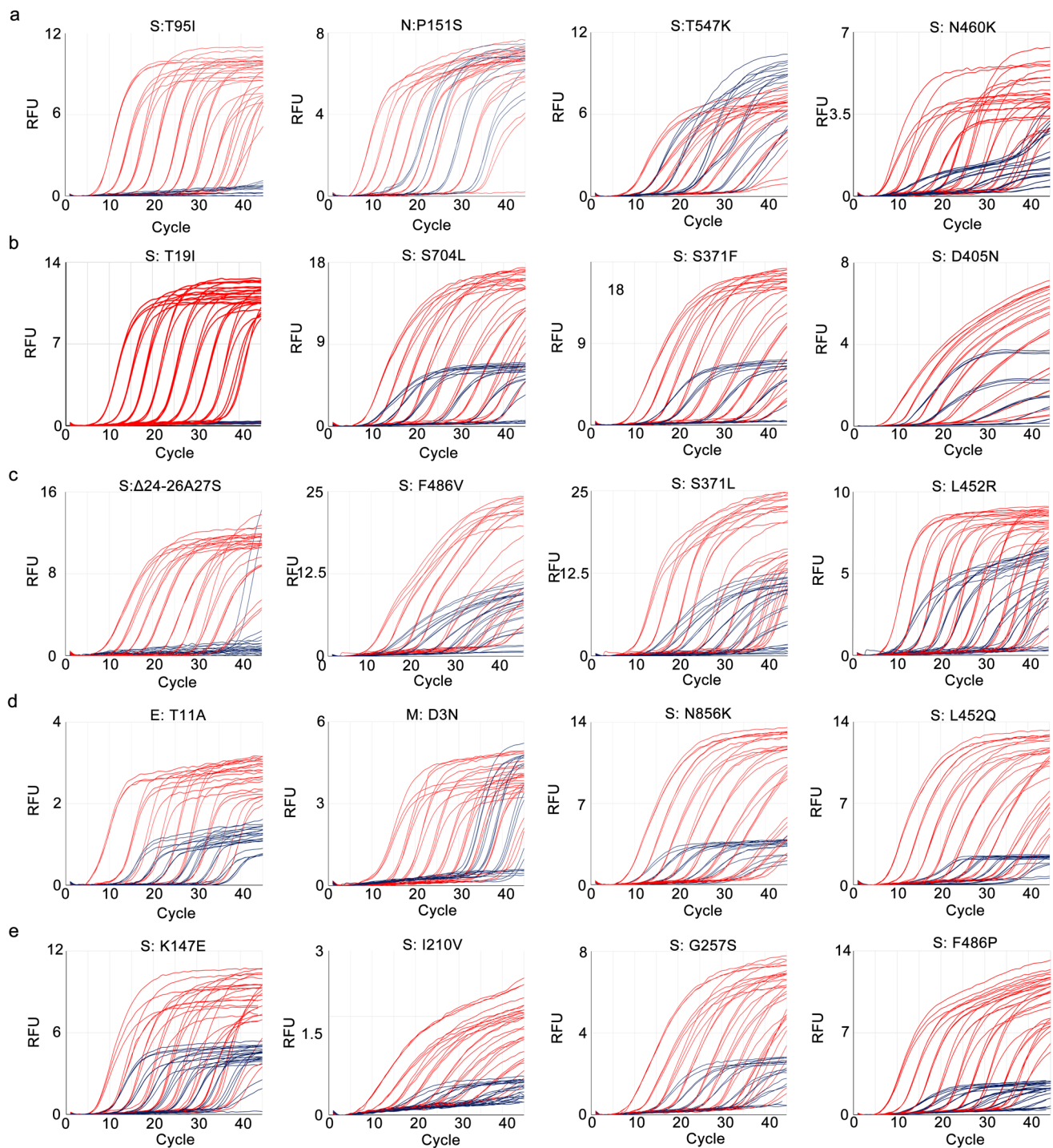
Fig. 3 Amplification curves for the developed multiplex allele-specific RT-qPCR assays against the mutated genes of SARS-CoV-2. The viral mutated genes covering all the mutations listed in Table 1 were in vitro transcribed and 10-fold diluted from 10^9 copies/reaction (8.45×10^9, 8.78×10^9, 6.95×10^9, and 2.33×10^9 for *nucleocapsid*, *envelope*, *membrane*, and *spike*, respectively) to 10^{-1} copies/reaction. Two parallel reactions targeting the prototype allele and the mutated allele of the developed assays were performed by using the in vitro transcribed and serially diluted mutated RNA as template. The amplification curves for the mutated allele-targeting reactions (in red) were then merged with those of the corresponding prototype allele-targeting reactions (in dark blue). RFU, relative fluorescence units, is a measurement of the fluorescence intensity generated from real-time PCR

Table 2 Absolute ΔCp values generated from the developed assays by using prototype template and mutated template, respectively

Assay		Allele	Coefficient of variation (CV) of Cp values for the 10-fold diluted in vitro transcribed prototype RNA template									
			10^{9*}	10^8	10^7	10^6	10^5	10^4	10^3	10^2	10^1	10^0
Prototype template	Assay 1	S: T95I	3.63	4.66	3.93	13.73	17.27	20.87	24.00	27.51	31.03	34.03
		N: P151S	2.22	8.65	9.31	9.02	11.02	11.97	9.85	24.42	27.47	30.68
		S: T547K	7.58	11.12	16.69	19.98	23.19	25.06	31.22	35.03	38.27	-
		S: N460K	2.24	2.37	2.45	3.12	3.25	3.55	3.88	3.65	6.68	37.29
	Assay 2	S: T19I	5.15	6.21	6.33	5.78	5.25	7.02	5.36	6.85	33.78	-
		S: S704L	3.21	4.67	4.10	3.02	2.45	30.34	33.75	36.60	38.70	-
		S: S371F	4.18	3.74	3.71	3.55	3.77	3.61	3.40	3.83	38.14	-
		S: D405N	3.01	3.49	3.11	4.69	4.39	4.17	-	-	-	-
	Assay 3	S: Δ24-26A27	3.62	4.16	4.53	4.43	4.74	5.19	5.38	5.63	34.76	36.59
		S: F486V	6.43	9.94	13.30	16.86	20.53	24.27	27.55	31.02	-	-
		S: S371L	28.11	10.93	14.18	17.67	21.26	25.00	28.29	31.75	35.54	-
		S: L452R	8.83	10.89	14.08	17.77	25.09	28.53	32.00	35.64	37.19	38.24
	Assay 4	E: T11A	6.89	10.26	13.52	16.58	19.75	23.05	26.56	29.91	33.26	36.71
		M: D3N	2.79	18.56	22.65	20.34	21.67	25.01	28.57	31.98	35.38	39.41
		S: N856K	11.65	11.26	12.36	19.44	13.52	14.69	29.77	34.07	-	-
		S: L452Q	3.34	12.89	17.25	18.63	20.72	24.47	28.00	31.74	35.23	-
	Assay 5	S: K147E	3.14	4.10	3.56	4.16	3.02	3.75	3.16	3.98	36.14	38.15
		S: I210V	7.56	8.20	7.66	8.03	7.61	5.86	6.45	29.87	34.31	35.65
		S: G257S	18.20	11.02	19.26	15.43	14.92	17.85	27.97	30.73	34.37	-
		S: F486P	3.76	3.55	3.52	4.67	3.22	3.94	3.58	31.52	34.67	37.11
Mutated template	Assay 1	S: T95I	7.45	11.03	14.58	18.10	22.28	24.90	31.52	34.67	-	-
		N: P151S	6.35	8.21	12.35	14.69	15.36	18.81	29.66	33.05	-	-
		S: T547K	2.90	3.31	5.62	2.65	6.12	7.58	32.69	35.07	-	-
		S: N460K	3.46	3.79	3.35	4.30	2.79	3.51	3.68	29.02	32.38	35.59
	Assay 2	S: T19I	8.51	11.76	15.08	18.59	21.93	25.68	29.39	33.23	36.17	37.25
		S: S704L	3.52	3.34	3.43	7.29	8.65	13.25	14.53	30.09	34.02	36.07
		S: S371F	3.39	6.21	12.03	14.69	16.62	22.36	25.63	29.18	31.50	35.24
		S: D405N	2.87	3.05	6.22	7.36	13.95	12.36	30.05	32.69	-	-
	Assay 3	S: Δ24-26A27	31.23	10.25	13.36	17.59	21.01	25.44	28.26	31.02	33.19	-
		S: F486V	2.88	5.36	3.27	5.61	4.28	2.48	3.02	36.68	39.24	-
		S: S371L	4.26	5.85	3.89	4.36	4.15	3.46	2.87	30.37	34.57	38.12
		S: L452R	3.31	3.56	3.22	3.47	4.44	4.02	5.21	2.98	35.44	38.01
	Assay 4	E: T11A	5.22	6.57	7.12	6.47	7.33	4.87	5.29	5.85	34.25	-
		M: D3N	20.22	19.38	15.20	14.11	14.68	28.19	30.81	33.47	36.42	-
		S: N856K	3.85	3.64	4.02	5.62	5.36	7.02	26.78	31.28	33.23	36.58
		S: L452Q	5.25	8.11	11.02	11.25	11.63	11.45	27.55	29.87	31.96	35.67
	Assay 5	S: K147E	3.58	3.46	3.88	4.02	4.26	5.14	4.68	4.01	30.45	34.60
		S: I210V	7.35	8.22	11.27	10.08	11.65	24.38	28.55	31.33	35.20	-
		S: G257S	5.47	6.25	6.24	5.45	6.58	9.59	4.68	31.45	33.25	38.47
		S: F486P	5.66	5.07	6.98	5.35	6.22	7.68	5.35	7.31	32.08	35.23

*The starting concentrations for the prototype genes of *nucleocapsid* (N), *envelope* (E), *membrane* (M), and *spike* (S) were 2.57×10^9, 4.28×10^9, 3.32×10^9, and 6.61×10^9 copies per reaction, respectively. The starting concentrations for the mutated genes of N, E, M, and S were 8.45×10^9, 8.78×10^9, 6.95×10^9, and 2.33×10^9 copies per reaction, respectively.

swabs were used to evaluate the clinical performance of the developed assays. Twenty-six of the 113 throat swabs were detected SARS-CoV-2 positive by a previous reported assay (Liu et al. 2020) and confirmed by Sanger sequencing, among which 25 were detected by the developed assays in the present study (including 7 BA.2.75, 5 BA.2.12.1, and 13 XBB.1). By
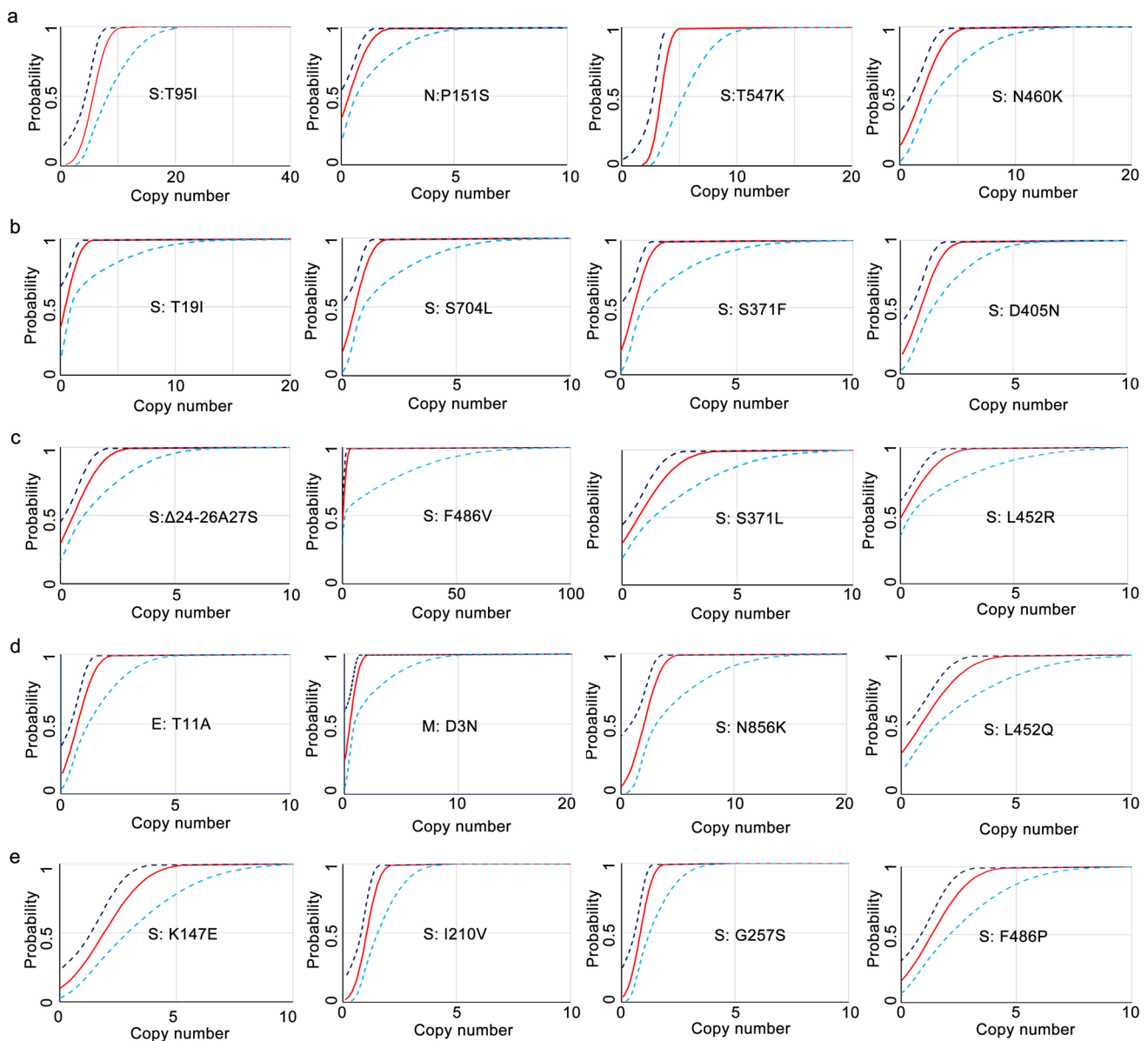
Fig. 4 Determination of limits of detection of the developed multiplex allele-specific RT-qPCR assays to detect the prototype RNA of SARS-CoV-2. Limits of detection (LoDs) for the developed RT-qPCR assays to detect the prototype RNA of SARS-CoV-2 were determined by the Probit regression (dose-response analysis) implemented in SPSS v22.0. RT-qPCR was performed by using the in vitro transcribed viral prototype RNA (2-fold diluted from 200 copies/reaction to 0.1 copies per reaction) as templates. The obtained Cp values and the corresponding copy number of viral RNA were applied for Probit Regression analysis. The inner solid line (in red) is a Probit curve. The outer dotted lines (in dark blue) are 95% CI (confidence interval)

comparing with Sanger sequencing (Table 5), the sensitivities of the developed assays were 92.86% for XBB.1 and 100% for the other enrolled Omicron subvariants and recombinant variants. The specificities of the developed assays were 99.07% for BA.2.75 and 100% for the other variants. The consistencies for BA.2.75, BA.2.12.1, and XBB.1 between the developed assays and Sanger sequencing were 99.12% (Kappa = 0.958, $P <$ 0.001), 100% (Kappa = 1.000, $P <$ 0.001), and 99.12% (Kappa = 0.929, $P <$ 0.001), respectively. These results suggested

good clinical performances of the developed multiplex allele-specific RT-qPCR assays.

Discussion

The distinct transmissibility among Omicron subvariants and potential impacts of the recombinant variants of SARS-CoV-2 call for quick viral variant screening method
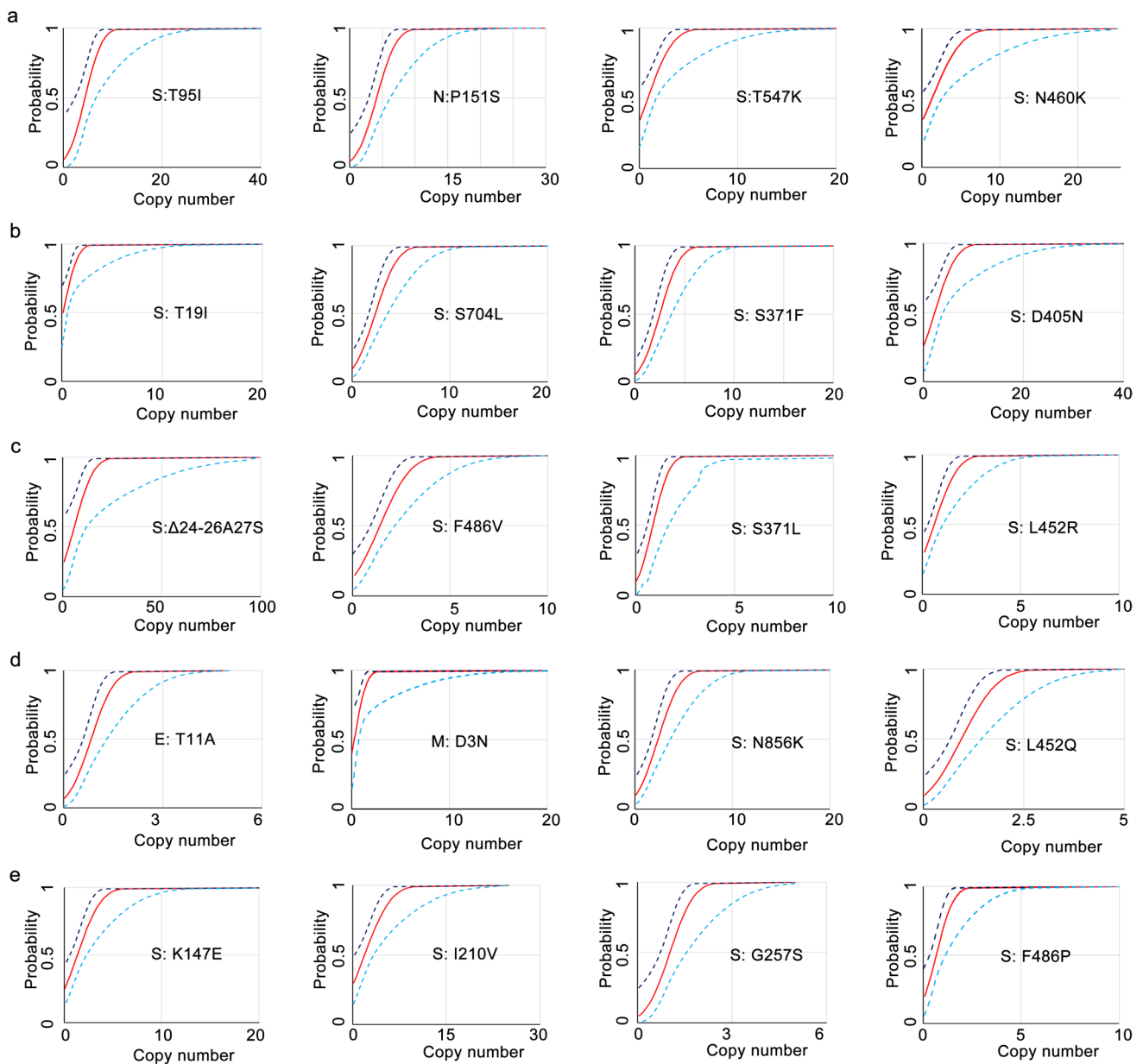
Fig. 5 Determination of limits of detection of the developed multiplex allele-specific RT-qPCR assays to detect the mutated RNA of SARS-CoV-2. Limits of detection (LoDs) for the developed RT-qPCR assays to the mutated RNA (covering all the alleles in Fig. 1c) of SARS-CoV-2 were determined by the Probit regression (dose-response analysis) implemented in SPSS v22.0. RT-qPCR was performed by using the in vitro transcribed mutated RNA (2-fold diluted from 200 copies/reaction to 0.1 copies per reaction) as templates. The obtained Cp values and the corresponding copy number of viral RNA were applied for Probit regression analysis

to effectively monitor the viral transmission (Carabelli et al. 2023). Allele-specific RT-qPCR is an easy-to-perform and wide applicable method in SNP screening (He et al. 2022), representing a potential basic technology for viral variant screening (Lee et al. 2022; Li et al. 2022). In the present study, we developed a panel of 5 multiplex allele-specific RT-qPCR assays targeting 20 key viral mutations for differentiation of SARS-CoV-2 Omicron subvariants (BA.1, BA.2, BA.4, BA.5, and their descendants) and related recombinant variants (XBB.1 and XBB.1.5). The redundant mutations for distinguishing viral subvariants were designed to avoid misinterpretation (because some of the mutations are shared by different viral variants) and to allow for observation of possible recombinant variant among Omicron subvariants.

Sequencing technologies have been applied for viral mutation screening. Among which, Sanger sequencing is the golden standard method to detect the rapidly emerging SARS-CoV-2 variants by providing a detailed view of

Table 3 Linear detection ranges and amplification efficiencies of the prototype allele targeting reactions in the developed multiplex allele-specific qRT-PCR assays

Assay	Allele	Cp values (mean ± s.d.) for 10-fold diluted in vitro transcribed prototype RNA template											R^2	Slope	Efficiency
		10^{9*}	10^8	10^7	10^6	10^5	10^4	10^3	10^2	10^1	10^0	10^{-1}			
Assay 1	S: T95I	6.37 ± 0.04	10.65 ± 0.04	13.73 ± 0.05	17.26 ± 0.06	20.86 ± 0.05	23.99 ± 0.05	27.50 ± 0.17	31.03 ± 0.15	34.02 ± 0.55	36.48 ± 0.36	-	0.9991	-3.09	110.68
	N: P151S	5.41 ± 0.19	8.70 ± 0.06	11.52 ± 0.09	15.17 ± 0.05	18.60 ± 0.01	21.08 ± 0.03	24.41 ± 0.21	27.47 ± 0.28	30.68 ± 0.09	33.07 ± 0.06	36.40 ± 0.20	0.9945	-3.45	94.92
	S: T547K	6.46 ± 0.09	11.16 ± 0.08	14.34 ± 0.04	18.07 ± 0.08	21.30 ± 0.01	23.23 ± 0.03	22.82 ± 0.39	32.27 ± 0.36	34.81 ± 0.54	37.29 ± 0.14	-	0.9963	-3.44	95.30
	S: N460K	6.65 ± 0.06	10.81 ± 0.04	13.97 ± 0.06	17.61 ± 0.02	21.21 ± 0.02	24.55 ± 0.04	28.24 ± 0.20	31.66 ± 0.06	34.45 ± 0.50	35.85 ± 0.58	-	0.9982	-3.36	98.44
Assay 2	S: T19I	5.50 ± 0.11	9.70 ± 0.16	12.24 ± 0.04	15.53 ± 0.03	19.07 ± 0.05	22.73 ± 0.12	26.18 ± 0.07	29.95 ± 0.08	33.37 ± 0.31	36.32 ± 0.41	37.49 ± 0.37	0.9972	-3.41	96.45
	S: S704L	8.80 ± 0.13	12.52 ± 0.04	15.88 ± 0.04	19.53 ± 0.08	23.05 ± 0.08	26.62 ± 0.05	30.33 ± 0.19	33.75 ± 0.42	36.59 ± 0.58	38.69 ± 1.19	-	0.9972	-3.97	94.17
	S: S371F	6.31 ± 0.16	10.49 ± 0.14	14.24 ± 015	17.95 ± 0.05	21.50 ± 0.06	25.26 ± 0.07	28.88 ± 0.04	32.28 ± 0.21	36.10 ± 0.29	38.13 ± 0.67	-	0.9979	-3.59	89.91
	S: D405N	5.51 ± 0.04	8.51 ± 0.13	12.00 ± 0.03	15.11 ± 0.08	19.80 ± 0.03	24.19 ± 0.07	28.36 ± 0.22	32.73 ± 0.08	36.69 ± 0.01	39.56 ± 0.46	-	0.9958	-3.33	99.66
Assay 3	S: Δ24-26Δ27	7.08 ± 0.07	10.69 ± 0.02	13.86 ± 0.05	17.39 ± 0.13	20.82 ± 0.05	24.56 ± 0.04	27.75 ± 0.04	31.13 ± 0.11	34.76 ± 0.30	36.59 ± 0.37	-	0.9991	-3.60	89.57
	S: F486V	6.43 ± 0.17	9.93 ± 0.03	13.29 ± 0.04	16.85 ± 0.06	20.52 ± 0.05	24.27 ± 0.02	27.54 ± 0.01	31.01 ± 0.05	34.75 ± 0.34	39.37 ± 0.16	-	0.9970	-3.47	94.17
	S: S371L	7.43 ± 0.03	10.92 ± 0.03	14.18 ± 0.05	17.67 ± 0.07	21.26 ± 0.05	24.99 ± 0.01	28.28 ± 0.03	31.74 ± 0.05	35.54 ± 0.39	36.88 ± 0.18	-	0.9971	-3.40	96.84
	S: L452R	6.76 ± 0.18	10.89 ± 0.05	14.07 ± 0.01	17.77 ± 0.08	21.33 ± 0.05	25.09 ± 0.05	28.52 ± 0.06	32.00 ± 0.18	35.64 ± 0.43	37.19 ± 0.56	-	0.9982	-3.37	98.03
Assay 4	E: T11A	10.25 ± 0.08	13.52 ± 0.14	16.57 ± 0.24	19.74 ± 0.08	23.05 ± 0.07	26.55 ± 0.07	29.90 ± 0.11	33.25 ± 0.16	36.71 ± 0.12	39.87 ± 0.65	-	0.9996	-3.44	95.30
	M: D3N	8.28 ± 0.14	11.51 ± 0.15	14.99 ± 0.02	18.17 ± 0.06	21.67 ± 0.07	25.01 ± 0.07	28.57 ± 0.09	31.98 ± 0.01	35.58 ± 0.01	39.41 ± 0.23	-	0.9993	-3.54	91.64
	S: N856K	7.57 ± 0.31	11.49 ± 0.05	14.49 ± 0.13	18.08 ± 0.15	21.63 ± 0.21	25.69 ± 0.21	29.76 ± 0.18	34.07 ± 1.36	37.26 ± 0.27	39.59 ± 0.52	-	0.9943	-3.32	100.08
	S: L452Q	7.26 ± 0.32	10.6 ± 0.29	13.51 ± 0.06	17.00 ± 0.03	20.72 ± 0.04	24.46 ± 0.06	28.00 ± 0.02	31.74 ± 0.04	35.23 ± 0.24	38.71 ± 0.29	-	0.9997	-3.32	100.08
Assay 5	S: K147E	8.43 ± 0.26	11.57 ± 0.05	15.68 ± 0.04	19.23 ± 0.01	22.72 ± 0.02	25.74 ± 0.03	28.99 ± 0.03	32.16 ± 0.11	36.13 ± 0.15	38.14 ± 0.14	-	0.9963	-3.64	88.25
	S: I210V	7.44 ± 0.08	11.51 ± 0.14	15 ± 0.04	18.71 ± 0.05	22.30 ± 0.20	26.34 ± 0.23	29.86 ± 0.18	34.30 ± 0.27	35.65 ± 0.18	38.26 ± 0.25	-	0.9968	-3.28	101.78
	S: G257S	6.55 ± 0.27	9.37 ± 0.1	13.02 ± 0.06	17.12 ± 0.05	20.14 ± 0.33	23.79 ± 0.29	27.97 ± 0.43	30.72 ± 0.32	34.37 ± 0.23	37.30 ± 1.17	-	0.9989	-3.49	93.43
	S: F486P	7.27 ± 0.23	11.03 ± 0.04	14.58 ± 0.06	18.1 ± 0.01	22.27 ± 0.01	24.89 ± 0.01	28.34 ± 0.12	31.51 ± 0.23	34.67 ± 0.33	37.11 ± 0.28	40.00 ± 0.00	0.9980	-3.36	98.44

*The starting concentrations for the prototype genes of *nucleocapsid* (N), *envelope* (E), *membrane* (M), and *spike* (S) were 2.57×10^9, 4.28×10^9, 3.32×10^9, and 6.61×10^9 copies per reaction, respectively

Table 4 Linear detection ranges and amplification efficiencies of the mutated allele targeting reactions in the developed multiplex allele-specific qRT-PCR assays

Assay	Allele	Cp values (mean ± s.d.) for 10-fold diluted in vitro transcribed mutated RNA template											R^2	Slope	Efficiency
		10^{9*}	10^8	10^7	10^6	10^5	10^4	10^3	10^2	10^1	10^0	10^{-1}			
Assay 1	S: T95I	4.05 ± 0.22	7.45 ± 0.14	11.03 ± 0.04	14.58 ± 0.06	18.1 ± 0.01	22.27 ± 0.01	24.89 ± 0.01	28.34 ± 0.12	31.51 ± 0.23	34.67 ± 0.33	37.11 ± 0.28	0.9968	−3.27	102.21
	N: P151S	2.56 ± 0.11	5.19 ± 0.06	8.92 ± 0.02	11.82 ± 0.07	15.17 ± 0.02	18.8 ± 0.02	22.48 ± 0.02	26.52 ± 0.09	29.66 ± 0.02	33.05 ± 0.28	34.66 ± 0.19	0.9992	−3.40	96.84
	S: T547K	4.06 ± 0.06	8.16 ± 0.15	12.07 ± 0.04	15.48 ± 0.06	19.09 ± 0.04	23.33 ± 0.05	25.97 ± 0.04	29.53 ± 0.09	32.69 ± 0.21	35.07 ± 0.28	36.74 ± 0.11	0.9921	−3.26	102.65
	S: N460K	4.52 ± 0.16	7.83 ± 0.15	11.29 ± 0.25	15.08 ± 0.04	18.42 ± 0.13	22.72 ± 0.06	25.51 ± 0.09	29.02 ± 0.06	32.38 ± 0.28	35.59 ± 0.18	39.6 ± 0.56	0.9970	−3.50	93.07
Assay 2	S: T19I	4.30 ± 0.12	8.51 ± 0.06	11.76 ± 0.04	15.08 ± 0.02	18.59 ± 0.03	21.92 ± 0.05	25.68 ± 0.04	29.39 ± 0.26	33.23 ± 0.26	36.17 ± 0.49	39.71 ± 0.49	0.9972	−3.58	90.25
	S: S704L	4.02 ± 0.09	8.05 ± 0.05	11.57 ± 0.05	14.92 ± 0.04	18.34 ± 0.05	21.84 ± 0.09	25.95 ± 0.13	30.09 ± 0.28	34.02 ± 0.2	36.7 ± 0.52	39.12 ± 1.51	0.9990	−3.60	89.57
	S: S371F	4.62 ± 0.19	8.87 ± 0.07	12.26 ± 0.05	15.68 ± 0.09	19.2 ± 0.03	22.86 ± 0.14	26.93 ± 0.17	30.86 ± 0.11	34.35 ± 0.51	37.07 ± 0.52	39.17 ± 1.43	0.9964	−3.51	92.71
	S: D405N	3.57 ± 0.21	7.89 ± 0.11	11.32 ± 0.03	14.75 ± 0.02	18.12 ± 0.05	21.28 ± 0.06	25.18 ± 0.04	29.4 ± 0.11	33.26 ± 1.23	36.27 ± 0.82	40.00 ± 0.05	0.9995	−3.51	92.71
Assay 3	S: Δ24-26Δ27	5.88 ± 0.10	9.01 ± 0.23	12.13 ± 0.09	15.2 ± 0.11	18.62 ± 0.12	22.69 ± 0.16	26.28 ± 0.01	29.84 ± 0.02	32.53 ± 0.24	35.05 ± 0.22	35.81 ± 0.18	0.9920	−3.27	102.21
	S: F486V	5.16 ± 0.13	8.75 ± 0.36	12.27 ± 0.06	15.42 ± 0.06	18.98 ± 0.1	23.17 ± 0.06	26.85 ± 0.04	30.32 ± 0.07	32.46 ± 0.22	35.14 ± 0.07	37.2 ± 0.06	0.9970	−3.47	94.17
	S: S371L	3.15 ± 0.11	6.63 ± 0.20	10.32 ± 0.11	13.26 ± 0.09	16.28 ± 0.18	19.8 ± 0.06	23.88 ± 0.06	27.66 ± 0.14	31.12 ± 0.17	33.18 ± 0.13	37.53 ± 0.31	0.9980	−3.43	95.68
	S: L452R	2.96 ± 0.15	6.76 ± 0.18	10.89 ± 0.05	14.07 ± 0.01	17.77 ± 0.08	21.33 ± 0.08	25.09 ± 0.05	28.52 ± 0.06	32.25 ± 0.18	35.64 ± 0.43	37.19 ± 0.56	0.9886	−3.19	105.82
Assay 4	E: T11A	7.45 ± 0.06	10.34 ± 0.26	13.67 ± 0.04	17.28 ± 0.04	20.62 ± 0.04	23.62 ± 0.05	27.03 ± 0.04	30.48 ± 0.03	33.88 ± 0.18	36.79 ± 0.14	39.5 ± 0.26	0.9996	−3.52	92.35
	M: D3N	6.68 ± 0.12	10.85 ± 0.13	14.84 ± 0.04	18.04 ± 0.04	21.64 ± 0.08	25.34 ± 0.16	28.98 ± 0.06	31.96 ± 0.06	35.58 ± 0.09	39.36 ± 0.17	-	0.9967	−3.42	96.06
	S: N856K	7.05 ± 0.08	11.35 ± 0.10	15.74 ± 0.22	19.25 ± 0.11	22.66 ± 0.14	26.28 ± 0.14	30.1 ± 0.29	33.8 ± 0.19	37.59 ± 0.11	39.63 ± 0.37	-	0.9976	−3.59	89.91
	S: L452Q	3.04 ± 0.13	5.23 ± 0.30	8.59 ± 0.06	11.96 ± 0.02	15.43 ± 0.07	20.24 ± 0.04	22.84 ± 0.09	26.66 ± 0.25	29.9 ± 0.18	32.37 ± 0.22	35.45 ± 0.34	0.9992	−3.27	102.21
Assay 5	S: K147E	4.15 ± 0.04	7.51 ± 0.03	11.04 ± 0.02	14.55 ± 0.02	17.98 ± 0.01	21.71 ± 0.14	24.94 ± 0.05	28.43 ± 0.08	31.72 ± 0.13	35.05 ± 0.92	-	0.9984	−3.38	97.63
	S: I210V	2.98 ± 0.06	5.25 ± 0.11	7.24 ± 0.08	11.56 ± 0.11	14.54 ± 0.08	18.62 ± 0.03	21.33 ± 0.08	24.76 ± 0.24	28.26 ± 0.24	31.56 ± 0.45	-	0.9988	−3.46	94.54
	S: G257S	4.12 ± 0.18	8.16 ± 0.15	12.07 ± 0.04	15.48 ± 0.06	19.09 ± 0.04	23.33 ± 0.05	25.97 ± 0.04	29.53 ± 0.09	32.69 ± 0.21	35.07 ± 0.28	-	0.9944	−3.30	100.92
	S: F486P	3.95 ± 0.15	7.33 ± 0.27	11.41 ± 0.24	15.36 ± 0.12	18.35 ± 0.29	22.36 ± 0.19	25.6 ± 0.39	28.84 ± 0.14	32.34 ± 0.14	35.24 ± 0.22	-	0.9987	−3.38	97.63

*The starting concentrations for the mutated genes of nucleocapsid (N), envelope (E), membrane (M), and spike (S) were 8.45×10^9, 8.78×10^9, 6.95×10^9, and 2.33×10^9 copies per reaction, respectively

Table 5 Clinical performance of the developed multiplex qRT-PCR assays for Omicron subvariants of SARS-CoV-2.

		The developed assays					
		BA.2.75		BA.2.12.1		XBB.1	
		Positive	Negative	Positive	Negative	Positive	Negative
Sanger sequencing	Positive	7	0	5	0	13	1
	Negative	1	105	0	108	0	100
Sensitivity (%)		100		100		92.86	
Specificity (%)		99.07		100		100	
Youden's index		0.9907		1.0000		0.9286	
PPV (%)		87.5		100		100	
NPV (%)		100		100		99	
Agreement (%)		99.12		100		99.12	
Kappa		0.958		1.000		0.929	
Sensitivity (%)		100		100		92.86	
Specificity (%)		99.07		100		100	

mutations (Wang et al. 2021). Nevertheless, Sanger sequencing is time-consuming, requiring a longer turnaround time to deal with, depending on expensive sequencer. Next-generation sequencing (NGS) based whole-genome sequencing (WGS) represents a promising strategy in searching viral mutations by providing a more comprehensive view of the viral genomic variations (Bull et al. 2020). However, the NGS-based WGS is costly and requires professional skills, making it hard for wide application especially in the developing areas (Simner et al. 2018). When facing the task of viral recombinant variant identification, the limitations of sequencing technologies are amplified, because sequencing of multiple genomic regions is required to reach a confirmed result.

RT-qPCR represents a promising approach in viral mutation screening with the advantages of time and cost-effective, easy to manage, and wide applicable (Corman et al. 2020). RT-qPCR-based short-amplicon high-resolution melting analysis (SA-HRM) has been applied for SARS-CoV-2 variant screening, allowing for cost-effective genotyping of single-nucleotide differences by the differential melting pattern of a short double-stranded DNA molecule (Diaz-Garcia et al. 2021). While SA-HRM is less specific and less robust than TaqMan assays, its results should be confirmed by TaqMan assays or DNA sequencing, making the overall processes time-consuming and costly.

Allele-specific RT-qPCR method provides an optimal strategy in screening viral mutations, which has been widely used for SNP screening (Cuenca et al. 2013; Gaudet et al. 2009; Ngai et al. 2010). Although several allele-specific RT-qPCR assays have been developed for the detection of SARS-CoV-2 variants either from clinical specimens (Borsova et al. 2021) or from wastewater (Graber et al. 2021), a comprehensive assay covering the current circulating Omicron subvariants and related

recombinant variants of SARS-CoV-2 is lacking. To meet this demand, we developed and analytically validated a panel of 5 multiplex allele-specific RT-qPCR assays for differentiation of SARS-CoV-2 Omicron subvariants and related recombinant variants. The developed assays exhibited better or comparable analytical sensitivities with the previously reported allele-specific RT-qPCR assays for SARS-CoV-2 variants (Borsova et al. 2021; Garson et al. 2022; Wang et al. 2021), indicating their potential value in screening current circulating SARS-CoV-2 variants.

As a potential shortcoming of the developed assays in this study, the unobserved or subsequently appeared mutations in the targeting area of the primers and probes could affect the performance of the assays by increasing the uncontrolled mismatch. To overcome this shortcoming, we select the unique mutations of the SARS-CoV-2 recombinant variants and the Omicron subvariants that are far away from the other existing viral mutations. Nevertheless, further evaluation is required to assess the potential influence of future mutations that occur in the targeting area of the primers and probes of the developed assays. Another potential shortcoming of the developed assays is a possible disturbance of result interpretation by the intra-/inter-assay Cp variation between the prototype allele targeting reaction and the mutated allele targeting reaction. Because all the intra- or inter-assay Cp variations were no more than 5% (Table 4 and Supplemental Table S3) (i.e., the highest variation of $Cp \leq 35 \times 5\% = 1.75$), and most of the Cp variations among intra- and inter-assay tests were caused by the inaccuracy in template dilution (which is not common in application of the developed assays in detecting clinical specimens), we thus set the threshold as $\Delta Cp > 2$ to avoid results misinterpretation induced by intra-/inter-assay Cp variations.

In summary, a panel of 5 multiplex allele-specific RT-qPCR assays were developed for differentiation of SARS-CoV-2 Omicron subvariants (BA.1, BA.2, BA.4, BA.5, and their descendants including BA.2.12.1, BA.2.10.1, BA.2.75, BA.2.76, BQ.1, and Ch.1.1) and related recombinant variants (XBF, XBB.1, and XBB.1.5). The developed assays exhibited excellent analytical sensitivities (LoDs: 1.47–18.52 copies per reaction), wide linear detections ranges (from 10^7 copies per reaction to 10^0 copies per reaction), good amplification efficiencies (88.25 to 110.68%), and excellent reproducibility (CVs < 5% in both intra-assay and inter-assay tests). The developed assays provide an alternative tool for quick differentiation of SARS-CoV-2 Omicron subvariants and related recombinant variants.

Declarations

Ethics approval The authors confirm that the ethical policies of the journal, as noted on the journal's author guidelines page, have been adhered to. No animals were used in this study.

Competing interests The authors declare no competing interests.

References

Becker SJ, Taylor J, Sharfstein JM (2021) Identifying and tracking SARS-CoV-2 variants - a challenge and an opportunity. N Engl J Med 385(5):389–391

Borsova K, Paul ED, Kovacova V, Radvanszka M, Hajdu R, Cabanova V, Slavikova M, Lickova M, Lukacikova L, Belak A, Roussier L, Kosticova M, Liskova A, Madarova L, Stefkovicova M, Reizigova L, Novakova E, Sabaka P, Koscalova A et al (2021) Surveillance of SARS-CoV-2 lineage B.1.1.7 in Slovakia using a novel, multiplexed RT-qPCR assay. Sci Rep 11(1):20494

Bull RA, Adikari TN, Ferguson JM, Hammond JM, Stevanovski I, Beukers AG, Naing Z, Yeang M, Verich A, Gamaarachchi H, Kim KW, Luciani F, Stelzer-Braid S, Eden JS, Rawlinson WD, van Hal SJ, Deveson IW (2020) Analytical validity of nanopore sequencing for rapid SARS-CoV-2 genome analysis. Nat Commun 11(1):6272

Carabelli AM, Peacock TP, Thorne LG, Harvey WT, Hughes J, Consortium C-GU, Peacock SJ, Barclay WS, de Silva TI, Towers GJ, Robertson DL (2023) SARS-CoV-2 variant biology: immune escape, transmission and fitness. Nat Rev Microbiol 21(3):162–177

Corman VM, Landt O, Kaiser M, Molenkamp R, Meijer A, Chu DK, Bleicker T, Brunink S, Schneider J, Schmidt ML, Mulders DG, Haagmans BL, van der Veer B, van den Brink S, Wijsman L, Goderski G, Romette JL, Ellis J, Zambon M et al (2020) Detection of 2019 novel coronavirus (2019-nCoV) by real-time RT-PCR. Euro Surveill 25(3):2000045

Cuenca J, Aleza P, Navarro L, Ollitrault P (2013) Assignment of SNP allelic configuration in polyploids using competitive allele-specific PCR: application to citrus triploid progeny. Ann Bot 111(4):731–742

Diaz-Garcia H, Guzman-Ortiz AL, Angeles-Floriano T, Parra-Ortega I, Lopez-Martinez B, Martinez-Saucedo M, Aquino-Jarquin G, Sanchez-Urbina R, Quezada H, Granados-Riveron JT (2021) Genotyping of the major SARS-CoV-2 clade by short-amplicon high-resolution melting (SA-HRM) analysis. Genes 12(4):531

Garson JA, Badru S, Parker E, Tedder RS, McClure MO (2022) Highly sensitive and specific detection of the SARS-CoV-2 Delta variant by double-mismatch allele-specific real time reverse transcription PCR. J Clin Virol 146:105049

Gaudet M, Fara AG, Beritognolo I, Sabatti M (2009) Allele-specific PCR in SNP genotyping. Methods Mol Biol 578:415–424

Germer S, Higuchi R (2003) Homogeneous allele-specific PCR in SNP genotyping. Methods Mol Biol 212:197–214

Graber TE, Mercier E, Bhatnagar K, Fuzzen M, D'Aoust PM, Hoang HD, Tian X, Towhid ST, Plaza-Diaz J, Eid W, Alain T, Butler A, Goodridge L, Servos M, Delatolla R (2021) Near real-time determination of B.1.1.7 in proportion to total SARS-CoV-2 viral load in wastewater using an allele-specific primer extension PCR strategy. Water Res 205:117681

He Q, Hu O, Chen M, Liang Z, Liang L, Chen Z (2022) A novel and cost-efficient allele-specific PCR method for multiple SNP genotyping in a single run. Anal Chim Acta 1229:340366

IBM Corp (2013) IBM SPSS statistics for windows. IBM Corp, Armonk, NY Version 22.0

Islam MR, Shahriar M, Bhuiyan MA (2022) The latest Omicron BA.4 and BA.5 lineages are frowning toward COVID-19 preventive measures: a threat to global public health. Health Sci Rep 5(6):e884

Kumar S, Stecher G, Tamura K (2016) MEGA7: molecular evolutionary genetics analysis version 7.0 for bigger datasets. Mol Biol Evol 33(7):1870–1874

Lee WL, Armas F, Guarneri F, Gu X, Formenti N, Wu F, Chandra F, Parisio G, Chen H, Xiao A, Romeo C, Scali F, Tonni M, Leifels M, Chua FJD, Kwok GW, Tay JY, Pasquali P, Thompson J et al (2022) Rapid displacement of SARS-CoV-2 variant Delta by Omicron revealed by allele-specific PCR in wastewater. Water Res 221:118809

Li J, Gao Z, Chen J, Cheng R, Niu J, Zhang J, Yang Y, Yuan X, Xia J, Mao G, Liu H, Dong Y, Wu C (2022) Development of a panel of three multiplex allele-specific qRT-PCR assays for quick differentiation of recombinant variants and Omicron subvariants of SARS-CoV-2. Front Cell Infect Microbiol 12:953027

Liu Y, Wang Y, Wang X, Xiao Y, Chen L, Guo L, Li J, Ren L, Wang J (2020) Development of two TaqMan real-time reverse transcription-PCR assays for the detection of severe acute respiratory syndrome coronavirus-2. Biosaf Health 2(4):232–237

Majumdar S, Sarkar R (2022) Mutational and phylogenetic analyses of the two lineages of the Omicron variant. J Med Virol 94(5):1777–1779

Ngai KL, Lam WY, Lee N, Leung TF, Hui DS, Chan PK (2010) Allele-specific conventional reverse-transcription polymerase

chain reaction as a screening assay for discriminating influenza a H1N1 (H275Y) oseltamivir-resistant and wild-type viruses. J Med Virol 82(8):1295–1298

Oude Munnink BB, Koopmans M (2023) Tracking SARS-CoV-2 variants and resources. Nat Methods 20(4):489–490

Raso A, Mascelli S, Nozza P, Ugolotti E, Vanni I, Capra V, Biassoni R (2011) Troubleshooting fine-tuning procedures for qPCR system design. J Clin Lab Anal 25(6):389–394

Rio DC, Ares M Jr, Hannon GJ, Nilsen TW (2010) Purification of RNA using TRIzol (TRI reagent). Cold Spring Harb Protoc 2010(6):pdb prot5439

Simner PJ, Miller S, Carroll KC (2018) Understanding the promises and hurdles of metagenomic next-generation sequencing as a diagnostic tool for infectious diseases. Clin Infect Dis 66(5):778–788

Srivastava S, Banu S, Singh P, Sowpati DT, Mishra RK (2021) SARS-CoV-2 genomics: an Indian perspective on sequencing viral variants. J Biosci 46(1):22

Wang H, Miller JA, Verghese M, Sibai M, Solis D, Mfuh KO, Jiang B, Iwai N, Mar M, Huang C, Yamamoto F, Sahoo MK, Zehnder J, Pinsky BA (2021) Multiplex SARS-CoV-2 genotyping reverse transcriptase PCR for population-level variant screening and epidemiologic surveillance. J Clin Microbiol 59(8):e0085921

Wolter N, Jassat W, Walaza S, Welch R, Moultrie H, Groome MJ, Amoako DG, Everatt J, Bhiman JN, Scheepers C, Tebeila N, Chiwandire N, du Plessis M, Govender N, Ismail A, Glass A, Mlisana K, Stevens W, Treurnicht FK et al (2022) Clinical severity of SARS-CoV-2 Omicron BA.4 and BA.5 lineages compared to BA.1 and Delta in South Africa. Nat Commun 13(1):5860

World Health Organization (2021) Tracking SARS-CoV-2 variants, contents updated on 28 Nov, 2021.https://www.who.int/activities/tracking-SARS-CoV-2-variants

Xiao Y, Li Z, Wang X, Wang Y, Wang Y, Wang G, Ren L, Li J (2021) Comparison of three TaqMan real-time reverse transcription-PCR assays in detecting SARS-CoV-2. J Virol Methods 288:114030

Yu J, Collier AY, Rowe M, Mardas F, Ventura JD, Wan H, Miller J, Powers O, Chung B, Siamatu M, Hachmann NP, Surve N, Nampanya F, Chandrashekar A, Barouch DH (2022) Neutralization of the SARS-CoV-2 Omicron BA.1 and BA.2 variants. N Engl J Med 386:1579–1580